Dietary cholesterol promotes steatohepatitis and liver tumorigenesis in HCV core gene transgenic mice

Xiaojing Wang[1,2], Naoki Tanaka[1,3], Xiao Hu[1,4], Takefumi Kimura[5], Yu Lu[1], Fangping Jia[1], Keiko Sato[6], Jun Nayayama[6], Kyoji Moriya[7], Kazuhiko Koike[8], and Toshifumi Aoyama[1]

[1]Department of Metabolic Regulation, Shinshu University School of Medicine, Matsumoto, Japan

[2]Department of Gastroenterology, Lishui Hospital, Zhejiang University School of Medicine, Lishui, Zhejiang, China

[3]Research Center for Social Systems, Shinshu University, Matsumoto, Japan

[4]Department of Pathophysiology, Hebei Medical University, People's Republic of China

[5]Department of Gastroenterology, Shinshu University School of Medicine, Matsumoto, Japan

[6]Department of Molecular Pathology, Shinshu University School of Medicine, Matsumoto, Japan

[7]Department of Infection Control and Prevention, The University of Tokyo, Tokyo, Japan

[8]Department of Gastroenterology, The University of Tokyo, Tokyo, Japan

Correspondence: Naoki Tanaka, M.D., Ph. D. Department of Metabolic Regulation, Shinshu University School of Medicine, 390-8621, Matsumoto, Japan

E-mail: naopi@shinshu-u.ac.jp;

Tel: +81-263-37-2851

Running title: Dietary cholesterol promotes steatohepatitis and HCC

Manuscript length: Total words 3316; Abstract words 212; Title (Characters with spaces) 89

Number of Figures and Tables: 6 figures and 1 supporting information.

Potential conflict of interest: The authors have declared that no conflict of interest exists.

Financial support: The authors have declared that no financial support exists.

Abbreviations:

4-HNE, 4-hydroxy-nonenal; ALT, alanine aminotransferase; AST, aspartate aminotransferase; ALP, alkaline phosphatase; αSMA, α-smooth muscle actin; Bax, BCL2-associated X protein; CCND1, cyclin D1; CDK4, cyclin-dependent kinase 4; CHOP, C/EBP homologous protein; CTGF, connective tissue growth factor; DR5, tumor necrosis factor receptor superfamily member 10b; ER, endoplasmic reticulum; FA, fatty acid; HCC, hepatocellular carcinoma; FXR, farnesoid X receptor; GAPDH, glyceraldehyde-3-phosphate dehydrogenase; HCV, hepatitis C virus; HCVcpTg, HCV core protein-expressing transgenic; LXR, liver X receptor; NAFLD, non-alcoholic fatty liver disease; NEFA, non-esterified FA; NF-κB, nuclear factor-kappa B; NQO1, NAD(P)H dehydrogenase quinine 1; NRF2, nuclear factor erythroid 2; OPN, osteopontin; PCNA, proliferating cell nuclear antigen; PPAR, peroxisome proliferator-activated receptor; qPCR, quantitative polymerase chain reaction; SREBP, sterol regulatory element-binding protein; T-Chol, total cholesterol; TG, triglyceride; TGF-β1, transforming growth factor β1; TLR, toll-like receptor.

Abstract

Previous epidemiological studies have suggested a link between high cholesterol intake and liver disease progression, including hepatocellular carcinoma (HCC). However, the precise mechanism of hepatotoxicity and hepatocarcinogenesis caused by excessive cholesterol consumption remains unclear. We aimed to investigate the impact of dietary cholesterol using hepatitis C virus core gene transgenic mice (HCVcpTg), which spontaneously developed HCC with age. Male HCVcpTg mice were treated for 15 months with either a purified control diet or an isocaloric diet containing 1.5% cholesterol, and liver phenotypes and tumor-associated signaling pathways were evaluated. The high-cholesterol diet-fed HCVcpTg mice exhibited a significantly higher incidence of liver tumors compared with the control diet mice (100% vs. 41%, $P < 0.001$). The diet induced steatohepatitis with pericellular fibrosis and evoked higher mRNA expression of pro-inflammatory and pro-fibrotic mediators along with greater oxidative and endoplasmic reticulum stress in the liver. Moreover, long-term consumption of cholesterol-rich diet activated nuclear factor-kappa B (NF-κB) and p62/sequestosome 1 (Sqstm1)-nuclear factor erythroid 2 (NRF2) axis, enhanced fibrogenesis, and consequently accelerated hepatic tumorigenesis. In conclusion, these results demonstrate that dietary cholesterol facilitates liver tumorigenesis by inducing steatohepatitis and up-regulating cellular stress and pro-inflammatory NF-κB and detoxifying p62/Sqstm1-NRF2 signals. Therefore, high dietary cholesterol should be limited in HCV-infected patients to prevent development of steatohepatitis, liver fibrosis, and HCC.

Keywords: steatohepatitis; NF-κB; p62/Sqstm1-NRF2 axis; fibrogenesis; oxidative stress

Introduction

Hepatocellular carcinoma (HCC) is the most common type of human cancer and is mainly caused by persistent infection of hepatitis B virus, hepatitis C virus (HCV), and high consumption of alcohol. In parallel with anti-viral therapies, avoidance of hepatotoxic substances, such as abstinence from alcohol[1], are required to protect liver, slow disease progression, and reduce the risk of liver cancer. Recently, obesity and overnutrition are growing risk factors of HCC worldwide[2]. It was reported that high-fat diet enhanced 7,12-dimethylbenz(a)anthracene-induced hepatocarcinogenesis through modulating microbiota[3], indicating the close relationship between dietary fat and liver tumor development. Clarifying the mechanism of hepatocarcinogenesis caused by specific lipids is important for preventing liver cancer.

Among various lipids, cholesterol is essential for forming cell/organella membranes. However, excessive cholesterol is deposited into vascular wall, leading to arteriosclerosis and ischemic cerebrocardiovascular disease. Cholesterol levels in humans are tightly regulated by two pathways: hepatic *de novo* synthesis from acetyl-CoA mainly regulated by hydroxymethylglutaryl-CoA (HMG-CoA) reductase and intestinal absorption from food. When dietary cholesterol is excessive, cholesterol absorption by enterocytes and *de novo* cholesterogenesis by hepatocytes are suppressed to maintain homeostasis[4-6]. The 2015-2020 Dietary Guidelines for Americans removed the recommendations of setting a limit to the maximum intake of 300 mg/day cholesterol, because there are no supporting evidence that dietary cholesterol increases circulating cholesterol and enhances the risk of cardiovascular disease[7].

However, it is natural to consider that dietary cholesterol can affect liver condition, since liver is a major organ of cholesterol metabolism. Indeed, previous large epidemiological studies have indicated an association between cholesterol intake and the outcome of liver disease. Ioannou et al.[8] showed that higher dietary cholesterol was associated with a greater incidence of cirrhosis and liver cancer in the U.S. general population. According to an analysis of clinical data obtained from the hepatitis C antiviral long-term treatment against cirrhosis (HALT-C) trial, higher

dietary cholesterol intake was significantly related to a higher risk of fibrosis progression, hepatic decompensation, and HCC[9]. Based on these results, it is postulated that dietary cholesterol possesses hepatotoxic and hepatocarcinogenic properties. However, estimation of cholesterol consumption from a dietary frequency questionnaire is not always identical to actual intake amount, and the precise mechanism regarding hepatotoxic effects of dietary cholesterol remains unclear.

To address this issue, we used HCV core gene transgenic mice (HCVcpTg). This mouse line exhibited spontaneous liver tumor development in approximately 30% of male mice between 16 and 18 months of age[10-13]. Since accompanying hepatitis or liver fibrosis were not observed[10-13], we considered that this mouse line is useful for assessing dietary cholesterol-induced hepatotoxicity. We hypothesized that high-cholesterol diet increased the prevalence of liver tumor in HCVcpTg mice, and treated them for 15 months with either a purified control diet or an isocaloric diet containing 1.5% cholesterol for the investigation of phenotypic changes.

Methods

Mice and treatment

HCVcpTg mice on a C57BL/6 genetic background were generated as described previously[10,11]. Male mice of 8-12 weeks old and weighing 25-30 g were used in this study. The mice were maintained in an animal facility under a standard conditions (25°C, 12-hour light/dark cycle, 4-5 mice/cage) with water *ad libitum*. The animals were randomly divided into two groups and fed either an AIN93G-based control diet (n = 17) or one containing 1.5% cholesterol diet (n = 13). The daily calorie amounts of the diets were identical. The detailed nutrient composition of the high-cholesterol diets is described elsewhere[14]. After the 15-month diet treatment period, the mice were sacrificed by CO_2 asphyxiation after six hours of fasting and serum and tissue samples were collected and stored at -80°C until use. All animal experiments were performed in accordance with the animal care guidelines approved by Shinshu University School of Medicine.

Biochemical analysis

Serum alanine aminotransferase (ALT), aspartate aminotransferase (AST), alkaline phosphatase (ALP), total bile acid (T-BA), total cholesterol (T-Chol), free cholesterol (F-Chol), triglyceride (TG), non-esterified fatty acid (NEFA), phospholipid (PC), and glucose were measured with commercially available enzyme assay kits (Wako Pure Chemical Industries, Ltd., Osaka, Japan). Serum insulin was determined by a mouse insulin ELISA kit (AKRIN-011T, Gunma, Japan). Total liver lipids were extracted according to the hexane:isopropanol method[15,16] and quantified using the same kits (Wako Pure Chemical Industries, Ltd.). For quantification of liver hydroxyproline content, frozen liver tissues (approximately 10 mg) were hydrolyzed in 6M HCl at 95°C for 20 hours. After cooling the samples to room temperature and centrifugation at 13,000 x *g* for 10 min, the supernatants were collected, diluted with deionized water to 4M HCl, and subsequently diluted 5-fold with deionized water to avoid the matrix effect. Hydroxyproline concentrations were measured using the QuickZyme Hydroxyproline Assay kit (QuickZyme BioSciences, Leiden, Netherlands) following

the manufacturer's protocol.

Histological analysis

Liver tissues were fixed in 10% neutral formalin, embedded in paraffin, cut into 4 μm sections, and stained with the hematoxylin and eosin or Azan-Mallory method[17]. Expression of pan-macrophage marker F4/80 and proliferating cell nuclear antigen (PCNA) was analyzed by immunohistochemistry[18]. Prior to anti-F4/80 immunostaining, deparaffinized liver sections were digested with 0.25% Difco trypsin 250 (BD Biosciences, San Jose, CA) at 37°C for 30 minutes. For the anti-PCNA antibody, deparaffinized liver sections were subjected to antigen retrieval by microwaving in 10 mM citrate buffer (pH 6.0) for 30 minutes. After blocking, liver sections were incubated for 1 hour with primary antibodies against F4/80 (CI-A3-1, Novus Biologicals, Centennial, CO; 1:100 dilution) or PCNA (sc-56, Santa Cruz Biotechnology, Dallas, TX; 1:100 dilution) at room temperature. Immunodetection was carried out using a Histofine® Simple Stain MAX PO (rat) Kit and Histofine® Mousestain Kit (both Nichirei Biosciences, Tokyo, Japan) for the anti-F4/80 and anti-PCNA antibodies, respectively. Peroxidase activity was visualized using a diaminobenzidine-H_2O_2 solution. Specific staining was not detected in control experiments omitting the primary antibody.

Analysis of mRNA expression

Total liver RNA was extracted with an RNeasy Mini Kit (Qiagen, Tokyo, Japan) and reverse-transcribed to cDNA using oligo-dT and random primers with the PrimeScript RT Reagent Kit (Perfect Real Time, Takara Bio Inc., Shiga, Japan). mRNA levels were measured by quantitative real-time polymerase chain reaction (qPCR) using THUNDERBIRD SYBR qPCR Mix (Toyobo Co, Ltd., Osaka, Japan) on an Applied Biosystems™ 7500 Fast Dx Real-Time PCR Instrument (Thermo Fisher Scientific, Waltham, MA). cDNA aliquots of 1 μg were added to each well. Specific primers were designed using the BLAST database released from the US National Library of Medicine and have been listed in Supplementary Table 1. mRNA levels were

calculated using the ΔΔCt method, normalized to 18S ribosomal RNA levels, and subsequently expressed as fold changes relative to those of HCVcpTg mice fed the control diet.

Immunoblot analysis

Whole liver lysates and hepatic nuclear fractions were prepared as described previously[12,13,19-21]. Protein concentrations were measured with a BCA Protein Assay Kit (Pierce, Rockford, IL). Lysate samples of 20-60 μg were separated by 10% sodium dodecyl sulfate-polyacrylamide gel electrophoresis (SDS-PAGE) and transferred onto polyvinylidene fluoride membranes (G9903119, Amersham, Freiburg, Germany) or nitrocellulose filter membranes (G9935264, Amersham). Non-specific reactions were blocked by 1-5% non-fat dry milk in Tris-buffered saline (1% Tween-20) for one hour at room temperature. The membranes were then incubated overnight with the primary antibodies listed in Supplementary Table 2. After washing four times, the membranes were incubated with horseradish peroxidase-conjugated secondary antibodies (115-035-003, Jackson ImmunoResearch Laboratories, West Grove, PA; 1:1000 dilution). Specific bands were detected using a myECL Imager System (Thermo Fisher Scientific). The positions of protein bands were determined by molecular weight with Prestained SDS-PAGE Standards (Bio-Rad, Hercules, CA). Band intensities were quantified using NIH ImageJ software (National Institutes of Health, Bethesda, MD), normalized to those of GAPDH or histone H1, and then expressed as fold changes relative to those of HCVcpTg mice fed the control diet.

Time course study

To examine the early changes in hepatic gene expression by dietary cholesterol overload, we tested samples obtained from male C57BL/6 wild-type mice treated with the 1.5% cholesterol diet or control diet for 2 months[14]. Hepatic mRNA levels were determined by qPCR.

Statistical analysis

All data are expressed as the mean ± standard error of the mean (SEM). The two-tailed unpaired Student's *t*-test was used for statistical analysis between the two groups. A *P* value of less than 0.05 was considered statistically significant.

Results

A high-cholesterol diet promotes steatohepatitis and hepatic tumorigenesis in HCVcpTg mice

The HCVcpTg mice were fed either a control diet or a 1.5% cholesterol diet for 15 months (Fig. 1A). Tumor prevalence was significantly higher in the high-cholesterol diet mice (13 of 13 mice, 100%) compared with the control diet mice (7 of 17 mice, 41%) (Fig. 1B). The liver-to-body weight ratio and serum ALT, AST, T-BA, and T-Chol values became significantly increased in the high-cholesterol diet mice over those in the control group (Fig. 1C and D, Supplementary Table 3). Hepatic content of TG, T-Chol, F-Chol, T-BA, NEFA, and PC were all significantly increased in the high-cholesterol diet mice as well (Fig. 1E and F, Supplementary Table 3). In agreement with these results, liver histology revealed marked macrovesicular steatosis and infiltration of inflammatory cells around steatotic hepatocytes, so-called crown-like appearance, in the high-cholesterol diet animals (Fig. 1G). The significant macrophage infiltration in the livers of high-cholesterol diet-fed mice was corroborated by enhanced mRNA levels of *Cd68*, a typical macrophage/monocyte marker, and increased F4/80-positive cells (Fig. 1G and 2A). These results demonstrates that a long-term high-cholesterol diet induced steatohepatitis and hepatic tumorigenesis in HCVcpTg mice.

Impact of high-cholesterol diet on hepatic lipid metabolism

To examine the changes in hepatic lipid metabolism caused by a cholesterol-rich diet, the expression of the genes involved in fatty acid (FA) and cholesterol metabolism was measured. There were no remarkable differences in the levels of mRNA encoding FA-catabolizing enzymes, which included medium- and long-chain acyl-CoA dehydrogenases (*Acadm* and *Acadl*, respectively) and acyl-CoA oxidase 1 (*Acox1*), all of which were also typical target genes of peroxisome proliferator-activated receptor (PPAR) α, between the test groups (Supplementary Fig. 1A). Similarly, no changes were detected in the mRNA levels of genes involved in *de novo* FA synthesis, such as FA synthase (*Fasn*), acetyl-CoA carboxylase α (*Acaca*), and stearoyl-CoA desaturase

1 (*Scd1*) (Supplementary Fig. 1A). The mRNA levels of *Cd36*, known to play a critical role in FA uptake from the blood, were significantly increased in the high-cholesterol diet mice (Supplementary Fig. 1B). The mRNA levels of genes encoding diacylglycerol O-acyltransferase 1 (*Dgat1*) and apolipoprotein B (*Apob*), respectively involved in TG incorporation and secretion from hepatocytes, were markedly increased. No changes were detected in the mRNA levels of genes involved in FA carriage/activation (*Fabp1* and *Acsl1*, encoding FA-binding protein 1 and acyl-CoA synthetase long-chain family member 1, respectively) or TG hydrolysis (*Pnpla2*, encoding patatin-like phospholipase domain containing 2) (Supplementary Fig. 1B). Overall, up-regulation of *Cd36* and *Dgat1* in the liver appeared to be responsible for more severe FA/TG accumulation and macrovesicular steatosis by a high-cholesterol diet.

In contrast, the mRNA levels encoding HMG-CoA synthase 1 and reductase (*Hmgcs1* and *Hmgcr*, respectively), conventional target genes of sterol regulatory element-binding protein 2 (SREBP2), were markedly suppressed by cholesterol-rich diet treatment (Supplementary Fig. 1C). Significant down-regulation was also detected in the mRNA levels encoding farnesyl-diphosphate farnesyltransferase 1 (*Fdft1*, also known as squalene synthase) and squalene epoxidase (*Sqle*), involved in cholesterol biosynthesis (Supplementary Fig. 1C). A high-cholesterol diet also increased the mRNA levels of ATP-binding cassette subfamily A member 1 (*Abca1*) and subfamily G member 8 (*Abcg8*), both target genes of liver X receptor (LXR) mobilizing cholesterol from the peripheral tissue and moderating cholesterol toxicity, as well as those of ATP binding cassette subfamily B member 11 (*Abcb11*), known to encode a bile salt export pump enhancing cholesterol excretion as bile acid (Supplementary Fig. 1C). These changes were considered as a normal adaptive response to dietary cholesterol overload.

A high-cholesterol diet activates NF-κB through TLR and inflammasome signaling

In order to investigate the mechanism of the enhanced inflammation in high-cholesterol diet-fed HCVcpTg mice, the expression of genes associated with

inflammatory signaling was assayed. The levels of mRNA encoding macrophage marker CD68 and such typical pro-inflammatory cytokines/chemokines as tumor necrosis factor-α (TNFα, encoded by *Tnf*), interleukin (IL)-1β (*Il1b*), chemokine (C-C motif) ligand 2 (*Ccl2*), and colony-stimulating factor 1 (*Csf1*) were significantly increased in the high-cholesterol diet-fed HCVcpTg mice (Fig. 2A). There were no remarkable differences in the mRNA levels of genes encoding arginase 1 (*Arg1*) or suppressor of cytokine signaling 3 (*Socs3*), respective indicators of M2 macrophage polarization and IL-6 downstream activation (Fig. 2A). In agreement with these findings, nuclear p65 and phosphorylated p65 levels were increased in high-cholesterol diet animals (Fig. 2B), indicating significant nuclear factor-κB (NF-κB) activation. The activation of Toll-like receptor (TLR) signaling and inflammasome were assessed as upstream signals of NF-κB. The levels of mRNAs encoding *Tlr2, Tlr4, Cd14*, and myeloid differentiation primary response gene 88 (*Myd88*), as well as TLR2 protein levels, were significantly increased in the cholesterol-rich diet mice (Fig. 2C and E). The mRNA levels of inflammasome-related genes, including NLR family pyrin domain containing 3 (*Nlrp3*), PYD and CARD domain containing (*Pycard*), pannexin 1 (*Panx1*), caspase 1 (*Casp1*), and absent in melanoma 2 (*Aim2*), were significantly increased by high-cholesterol diet treatment (Fig. 2D). Pro-caspase 1 and cleaved caspase 1 protein levels were determined by immunoblot analysis since caspase 1 processing is crucial for inflammasome activation. Both forms of caspase 1 were markedly increased in the livers of cholesterol-rich diet-fed mice (Fig. 2E). These results demonstrated that dietary cholesterol activated NF-κB mainly due to activation of TLR signaling and inflammasomes.

A high-cholesterol diet promotes liver fibrogenesis

Not only inflammation, but also ensuing fibrogenesis plays an important role in oncogenesis. Indeed, significantly higher levels of mRNA encoding transforming growth factor (TGF)-β1 (*Tgfb1*), α-smooth muscle actin (αSMA, encoded by *Acta2*), and collagen 1a1 (*Col1a1*) were observed in high-cholesterol diet HCVcpTg mice

compared with controls (Fig. 3A). The mRNA levels of genes encoding connective tissue growth factor and galectin 3 (encoded by *Ctgf* and *Lgals3*, respectively), both key drivers of fibrogenesis, were also increased in high-cholesterol diet mice (Fig. 3A). Immunoblot analysis of αSMA (Fig. 3B), hepatic hydroxyproline contents (Fig. 3C), and Azan-Mallory staining (Fig. 3D) all corroborated that dietary cholesterol markedly enhanced fibrogenesis.

A high-cholesterol diet enhances oxidative and endoplasmic reticulum (ER) stress, leading to lipoapoptosis.

Since cellular stress accelerates the inflammation-fibrosis-cancer axis, the severity of oxidative and ER stress was determined. The levels of mRNA encoding reactive oxygen species (ROS)-generating enzymes, such as NADPH oxidase 2 (*Cybb*) and p47phox (*Ncf1*), were significantly increased in high-cholesterol diet mice (Fig. 4A). As an adaptive response, the mRNA levels of oxidative stress-ameliorating enzymes, including NADPH quinone dehydrogenase 1 (NQO1, encoded by *Nqo1*) and heme oxygenase 1 (*Hmox1*), were also increased (Fig. 4A). NQO1 protein levels and amounts of 4-hydroxy-nonenal (4-HNE), a major lipid peroxidation aldehyde, were markedly raised in the liver of high-cholesterol diet HCVcpTg mice (Fig. 4B and C), corroborating enhanced hepatic oxidative stress by high cholesterol intake.

The mRNA levels of ER stress-induced gene DNA-damage inducible transcript 3 (*Ddit3*) and the encoding CHOP protein levels were significantly increased in the high-cholesterol diet mice (Fig. 4A and B). Oxidative and ER stress stimulate lipoapoptosis. Accordingly, the mRNA levels of genes encoding pro-apoptotic mediators, such as death receptor 5 (DR5, encoded by *Tnfrsf10b*) and B cell leukemia/lymphoma (BCL) 2-associated X protein (*Bax*), were enhanced in these mice (Fig. 4A) without any alterations in the mRNA encoding anti-apoptotic *Bcl2 and Bcl2l1* (data not shown). Increased DR5 and BAX by a high-cholesterol diet were confirmed by immunoblot analysis (Fig. 4B). Collectively, dietary cholesterol caused greater oxidative and ER stress in the liver of HCVcpTg mice, implicating in aggravated hepatocyte damage and hepatic inflammation/fibrosis.

Impact of cholesterol-rich diet on liver cell division and stemness

Since the sustained acceleration of hepatocyte proliferation may promote the development of liver tumors, the expression of cell cycle regulators was assessed. The mRNA levels of PCNA were significantly elevated in the high-cholesterol diet HCVcpTg mice (Fig. 5A), which was confirmed at the protein levels by immunoblot analysis and immunostaining (Fig. 5B and C). Irrespectively of the increased mRNA levels of p53, a well-known tumor suppressor gene (Fig. 5A), other key cell cycle regulators, including myelocytomatosis oncogene (*Myc*), cyclin D1 (*Ccnd1*), cyclin-dependent kinase 4 (*Cdk4*), and p21, did not exhibit meaningful differences (Fig. 5A). The mRNA expressions of such cancer stemness markers as epithelial cell adhesion molecule (*Epcam*), prominin 1 (*Cd133*), *Cd44*, and aldehyde dehydrogenase 1 family member A1 (*Aldh1a1*) tended to increase by a high-cholesterol diet but did not reach statistical significance (Fig. 5D). Therefore, dietary cholesterol overload appeared to enhance PCNA expression and drive cell proliferation. This disruption of cell division may have accelerated the dietary cholesterol-cancer axis.

A cholesterol-rich diet causes p62/Sqstm1-NRF2 activation

The activation of the p62/sequestosome 1 (Sqstm1, encoded by *Sqstm1*)-nuclear factor erythroid 2 (NRF2, encoded by *Nfe2l2*) axis is a recently proposed mechanism of hepatocarcinogenesis[22,23]. Indeed, marked amplification of p62 and NRF2 expression and increased nuclear NRF2 content were detected in high-cholesterol diet mice (Fig. 6A-C), which indicated significant activation of p62/Sqstm1-NRF2 detoxifying axis to likely promote liver tumorigenesis.

Short-term cholesterol-rich diet treatment stimulates inflammatory signaling

Lastly, in order to determine which pathways were initially activated by cholesterol-rich diet feeding prior to liver tumor development, hepatic mRNA levels of representative genes were quantified in 2-month cholesterol-rich diet-fed mice exhibiting no tumors in the body. The mRNA levels of genes associated with

inflammation (*Cd68, Ccl2,* and *Tlr2*) and hepatocyte proliferation (*Pcna*) were elevated even by 2-month cholesterol diet feeding, while those of genes involved in ER stress (*Ddit3*), fibrogenesis (*Acta2* and *Col1a1*), and p62/Sqstm1-NRF2 signaling were unchanged (Supplementary Fig. 2). Thus, enhanced inflammatory signaling and hepatocyte division appeared to be early events following dietary cholesterol overload.

Discussion

Several epidemiological reports have shown an association between high dietary cholesterol intake and an elevated risk of liver disease progression[24-26], although the direct relationship and precise mechanism remain undetermined. The current study provides supportive evidence that a cholesterol-rich diet induces steatohepatitis and a significantly higher prevalence of liver tumor in HCVcpTg mice. Comprehensive mechanistic investigation revealed that increased cellular stress, activated NF-κB and p62/Sqstm1-NRF2, and enhanced liver fibrogenesis represented a central pathway for liver tumorigenesis in HCVcpTg mice treated with a high-cholesterol diet for 15 months. Based on our results, we propose a novel mechanism on how dietary cholesterol overload promotes liver tumorigenesis (Fig. 6D).

Disrupted lipid metabolism is frequently associated with HCC development. For example, several studies showed overexpression of FA-synthesizing enzymes, which were mainly regulated by SREBP-1c, in HCC patients[27-30]. It has also been documented that activation of PPARα, a master regulator of FA catabolism, causes HCC in mice[13]. A positive link of oncogenic forkhead Box M1 expression with *Srebp2* activation and anti-tumor properties of *Lxr* was reported as well[31]. However, we observed that the expression of SREBP-1c/PPARα target genes were unchanged, SREBP2 was down-regulated, and LXR was up-regulated in the high-cholesterol diet HCVcpTg mice. These results prompted us to consider a novel mechanism of liver tumorigenesis independently of SREBP, PPARα, and LXR. Additionally, *Sqle* has been reported as an important driver of fatty liver-related HCC. This enzyme was overexpressed in HCC of diethylnitrosamine-primed mice with high-fat high-cholesterol diet, and forced expression of this enzyme promote cellular proliferation in hepatocytes[32,33]. However in this study, *Sqle* was markedly down-regulated by dietary cholesterol loading, likely due to physiological compensation. It seemed that *Sqle* overexpression was not associated with enhanced liver tumorigenesis observed in high-cholesterol diet-treated HCVcpTg mice.

Long-term dietary cholesterol overload increases both total and free cholesterol content in the liver. Several molecular mechanisms have been proposed for the

hepatotoxicity caused by cholesterol accumulation. Increased free cholesterol directly aggravates the integrity and fluidity of mitochondrial and ER membranes, causing mitochondrial/ER dysfunction and increased oxidative and ER stress[34,35]. Cholesterol also activates inflammasomes to form crystals and can be a potent ligand for TLR2/4. These pathological characteristics resulted in persistent activation of NF-κB in the liver, ultimately leading to liver fibrosis and HCC.

The most remarkable finding in this study was that dietary cholesterol caused activation of the p62/Sqstm1-NRF2 detoxifying pathway, a key contributor to the progression from premalignant changes to HCC[22,23,36]. p62/Sqstm1 is an ubiquitin-binding autophagy receptor and signaling protein that accumulates in pre-malignant liver disease and HCC. p62 is detected in Mallory-Denk bodies and localizes in ballooned hepatocytes, which are frequently found in non-alcoholic steatohepatitis (NASH), alcoholic steatohepatitis, and HCC[37]. The overexpression of p62/Sqstm1 promotes NRF2-mediated metabolic reprogramming, thus conferring resistance to anti-cancer agents, immortalization, and auto-proliferative tumor properties. As far as we know, this is the first study demonstrating p62/Sqstm1-NRF2 pathway activation due to a cholesterol-rich diet. Since the p62/Sqstm1-NRF2 axis is considered a novel target for HCC, restriction of dietary cholesterol might be useful for preventing the disease through suppression not only of NF-κB, but also of p62/Sqstm1-NRF2.

In the present study, a 15-month 1.5% cholesterol-containing diet resulted in macrovesicular steatosis, infiltration of inflammatory cells around steatotic hepatocytes, and pericellular fibrosis, all which were hallmarks of NASH. The test diet used in this investigation was isocaloric to the control diet with an elevation in cholesterol. It is difficult to reproduce the pathological features of NASH in mice using a regular high-fat diet without cholesterol supplementation[38.39]. A cholesterol-rich diet can induce the activation of Kupffer cells and hepatic stellate cells[40-42]. Thus, this study allowed us to confirm the importance of dietary cholesterol in NASH development.

Prolonged excessive dietary cholesterol consumption facilitates liver

tumorigenesis by activating several oncogenic pathways, such as NF-κB and the p62/Sqstm1-NRF2 axis. Short-term high-cholesterol treatment study revealed that enhanced inflammatory signaling and PCNA overexpression were early events during liver tumorigenesis induced by dietary cholesterol overload. Although the finding that a cholesterol-rich diet augmented PCNA expression is intriguing, its precise mechanism requires elucidation in future investigations. Since cholesterol is a precursor of steroid hormone, a high-cholesterol diet may disrupt steroid hormone metabolism and consequently promote hepatocyte division.

In conclusion, the present study provides novel information regarding a mechanistic link between dietary cholesterol overload and HCV core protein-induced liver tumorigenesis through the up-regulation of specific oncogenic signals. Dietary cholesterol should be limited to prevent development of steatohepatitis, liver fibrosis, and HCC. Further studies are needed to clarify the impact of dietary cholesterol in other models of hepatocarcinogenesis to generalize the findings uncovered in this investigation.

Acknowledgment

We appreciate Mr. Trevor Ralph for his English editorial assistance and thank Dr. Takero Nakajima and Dr. Ruan Guo (Shinshu University School of Medicine) for their invaluable help, advice, instruction, and encouragement.

Author contribution

Design and writing the paper: NT and TA

Performing experiments: XW, NT, XH, TK, YL, FJ, and KS

Analyzing data: XW, NT, XH, TK, YL, and KS

Supervision: NJ, KM, and KK

All authors read and approved the final manuscript.

Figure Legends

Fig. 1. Higher tumor prevalence and development of steatohepatitis in the liver of HCVcpTg transgenic mice after a 15-month high-cholesterol diet.

(A) Male 8-week-old C57BL/6 HCVcpTg mice were treated with a 1.5% cholesterol-containing diet (n = 13) or a control AIN93G diet (n = 17) for 15 months.

(B) Liver tumor prevalence.

(C) Liver weight (LW) expressed as a percentage of body weight (BW).

(D-F) Serum ALT activities and liver content of triglycerides (TG) and total cholesterol (T-Chol).

(G) Representative histological appearance of the liver. Hematoxylin and eosin staining (HE) and F4/80 immunostaining; Bar = 50 μm (100x magnification) or 20 μm (400x magnification). The liver of high-cholesterol diet mice showed abundant large lipid droplets in hepatocytes and infiltration of inflammatory cells around steatotic hepatocytes (yellow box) showing a crown-like appearance. The inflammatory cells were positive for F4/80.

Values are expressed as mean ± SEM. $*P < 0.05$, $**P < 0.01$, $***P < 0.001$ between control diet and high-cholesterol diet HCVcpTg mice.

Figure 1

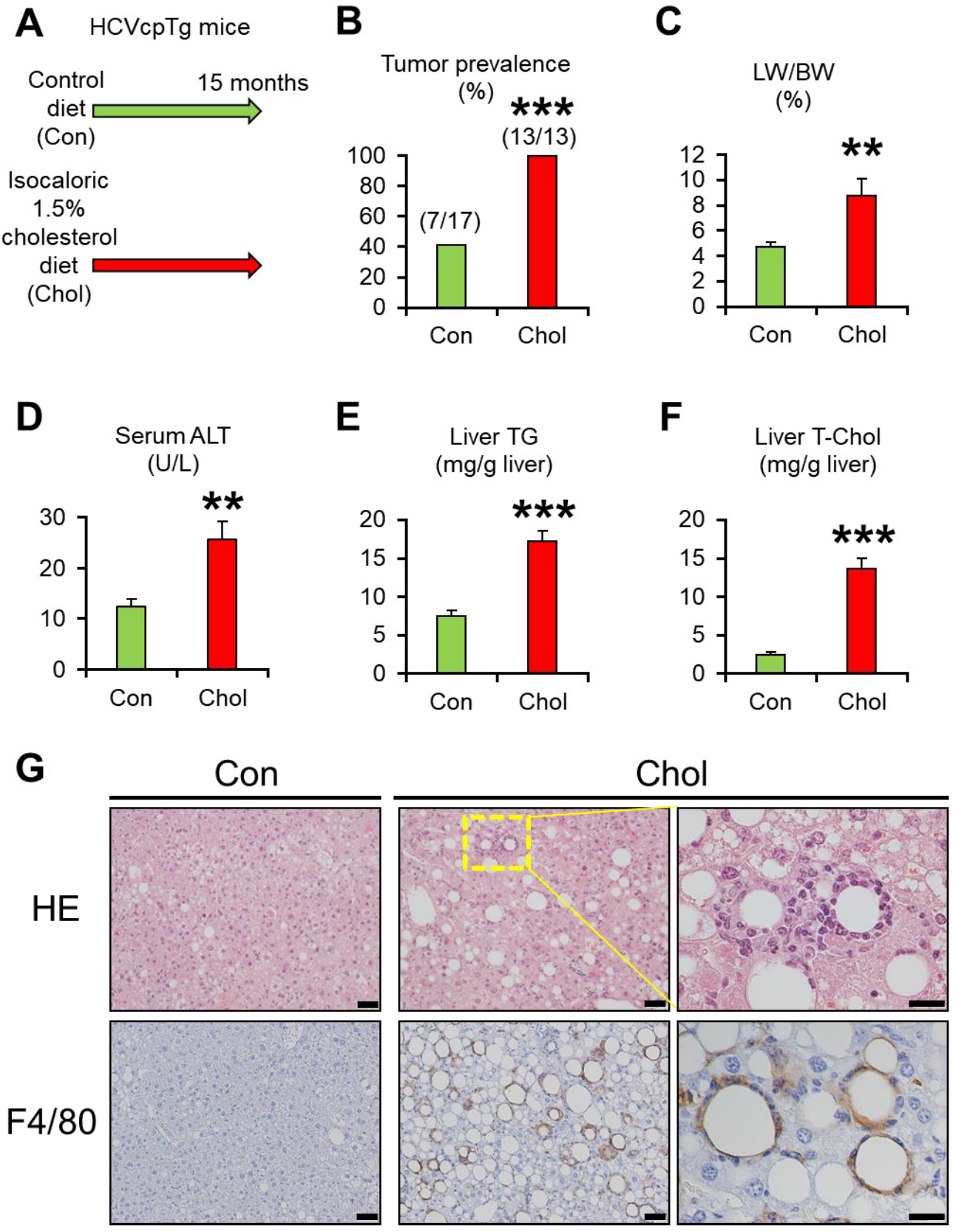
A
HCVcpTg mice
Control diet (Con)
15 months
Isocaloric 1.5% cholesterol diet (Chol)
B
Tumor prevalence (%)
***
(13/13)
(7/17)
100
80
60
40
20
0
Con
Chol
C
LW/BW (%)
**
12
10
8
6
4
2
0
Con
Chol
D
Serum ALT (U/L)
**
30
20
10
0
Con
Chol
E
Liver TG (mg/g liver)
***
20
15
10
5
0
Con
Chol
F
Liver T-Chol (mg/g liver)
***
20
15
10
5
0
Con
Chol
G
Con
Chol
HE
F4/80

Fig. 2. Aggravated hepatic inflammation in the liver of HCVcpTg transgenic mice after a 15-month high-cholesterol diet.

(A) qPCR analysis of genes associated with inflammation.

(B) Immunoblot analysis of NF-κB p65 and phosphorylated p65 (p-p65). Liver nuclear fractions (20 μg of protein) were loaded into each well. The band of histone H1 was used as a loading control. Band intensities were measured densitometrically, normalized to those of the loading controls, and subsequently expressed as values relative to those of control diet mice. Results were obtained from two independent immunoblot experiments.

(C) qPCR analysis of genes associated with TLRs.

(D) qPCR analysis of genes associated with inflammasomes.

(E) Immunoblot analysis of TLR2 and caspase 1. Whole liver homogenates (45 μg of protein) were loaded into each well. The caspase 1 antibody could detect pro-caspase 1 and cleaved (activated) caspase 1. The band of GAPDH was used as a loading control. Band intensities were measured densitometrically, normalized to those of the loading controls, and subsequently expressed as values relative to those of control diet mice. Results were obtained from two independent immunoblot experiments.

All mRNA levels were normalized to 18S mRNA levels and subsequently expressed as values relative to those of control diet mice. Values are expressed as the mean ± SEM. $*P < 0.05$, $**P < 0.01$, $***P < 0.001$ between control diet and high-cholesterol diet HCVcpTg mice.

Figure 2

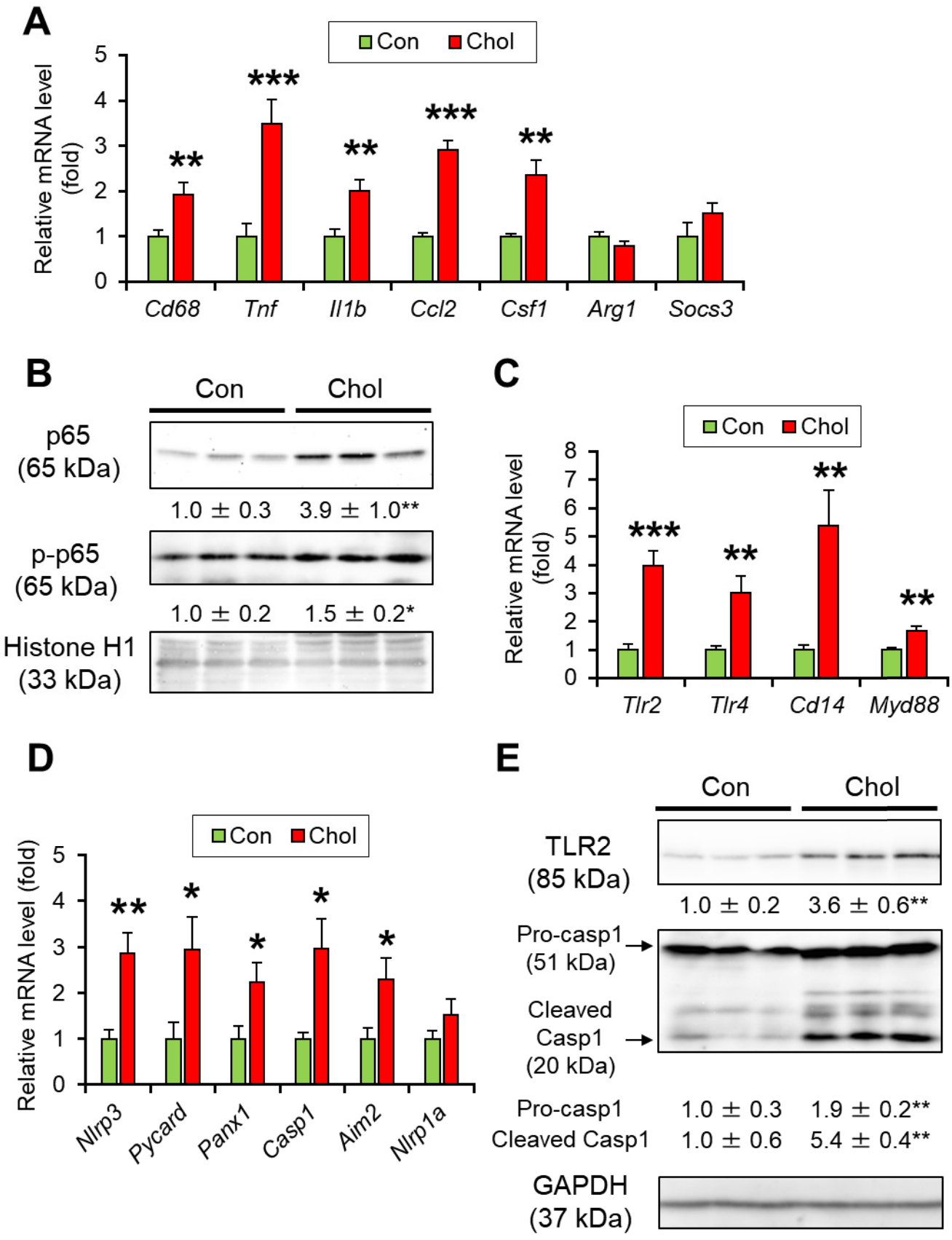
A
Con
Chol
Relative mRNA level (fold)
0
1
2
3
4
5
**
***
**
***
**
Cd68
Tnf
Il1b
Ccl2
Csf1
Arg1
Socs3
B
Con
Chol
p65 (65 kDa)
1.0 ± 0.3
3.9 ± 1.0**
p-p65 (65 kDa)
1.0 ± 0.2
1.5 ± 0.2*
Histone H1 (33 kDa)
C
Con
Chol
Relative mRNA level (fold)
0
1
2
3
4
5
6
7
8
***
**
**
**
Tlr2
Tlr4
Cd14
Myd88
D
Con
Chol
Relative mRNA level (fold)
0
1
2
3
4
5
**
*
*
*
*
Nlrp3
Pycard
Panx1
Casp1
Aim2
Nlrp1a
E
Con
Chol
TLR2 (85 kDa)
1.0 ± 0.2
3.6 ± 0.6**
Pro-casp1 (51 kDa)
Cleaved Casp1 (20 kDa)
Pro-casp1
1.0 ± 0.3
1.9 ± 0.2**
Cleaved Casp1
1.0 ± 0.6
5.4 ± 0.4**
GAPDH (37 kDa)

Fig. 3. More severe fibrosis in the liver of HCVcpTg transgenic mice after a 15-month high-cholesterol diet.

(A) qPCR analysis of genes associated with liver fibrosis.

(B) Immunoblot analysis of αSMA. Whole liver homogenates (45 μg of protein) were loaded into each well. The bands of GAPDH were used as the loading control. Band intensities were measured densitometrically, normalized to those of the loading control, and expressed as values relative to those of control diet mice. Results were obtained from two independent immunoblot experiments.

(C) Hepatic hydroxyproline content.

(D) Representative photomicrographs of Azan-Mallory staining. Bar = 50 μm (100x magnification). Dense pericellular/periportal fibrosis was detected in the high-cholesterol diet HCVcpTg mice.

All mRNA levels were normalized to 18S mRNA levels and subsequently expressed as values relative to those of control diet mice. Values are expressed as mean ± SEM. $*P < 0.05$, $**P < 0.01$, $***P < 0.001$ between control diet and high-cholesterol diet HCVcpTg mice.

Figure 3

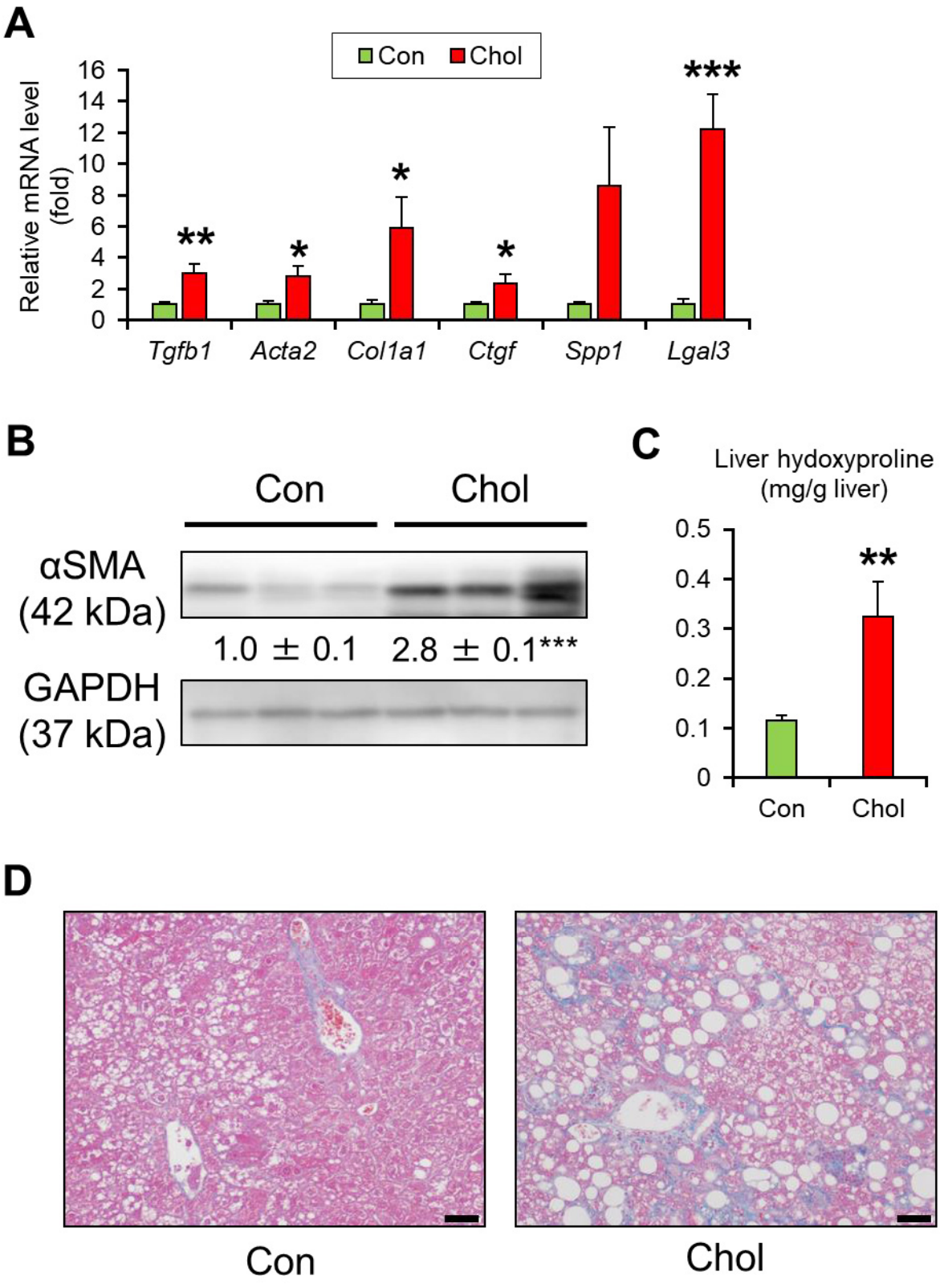
A
Con
Chol
Relative mRNA level (fold)
16
14
12
10
8
6
4
2
0
**
*
*
*
***
Tgfb1
Acta2
Col1a1
Ctgf
Spp1
Lgal3
B
Con
Chol
αSMA (42 kDa)
1.0 ± 0.1
2.8 ± 0.1***
GAPDH (37 kDa)
C
Liver hydoxyproline (mg/g liver)
0.5
0.4
0.3
0.2
0.1
0
**
Con
Chol
D
Con
Chol

Fig. 4. Greater oxidative stress, ER stress, and apoptotic signaling in the liver of HCVcpTg transgenic mice after a 15-month high-cholesterol diet.

(A) qPCR analysis of genes associated with oxidative stress (*Cybb, Ncf1, Nqo1* and *Hmox1*), ER stress (*Ddit3*), and cell stress-associated pro-apoptotic signaling *(Tnfrsf10b, Bax*). All mRNA levels were normalized to 18S mRNA levels and subsequently expressed as values relative to those of control diet mice.

(B and C) Immunoblot analysis of oxidative stress-associated protein NQO1, ER stress-associated protein CHOP, cell stress-associated pro-apoptotic proteins DR5 and BAX (B), and 4-HNE, a major lipid peroxidation aldehyde (C). Whole liver homogenates (45-60 μg of protein) were loaded into each well. The bands of GAPDH was used as the loading control. Band intensities were measured densitometrically, normalized to those of the loading control, and expressed as values relative to those of control diet mice. Results were obtained from two independent immunoblot experiments.

Values are expressed as mean ± SEM. $*P < 0.05$, $**P < 0.01$, $***P < 0.001$ between control diet and high-cholesterol diet HCVcpTg mice.

Figure 4

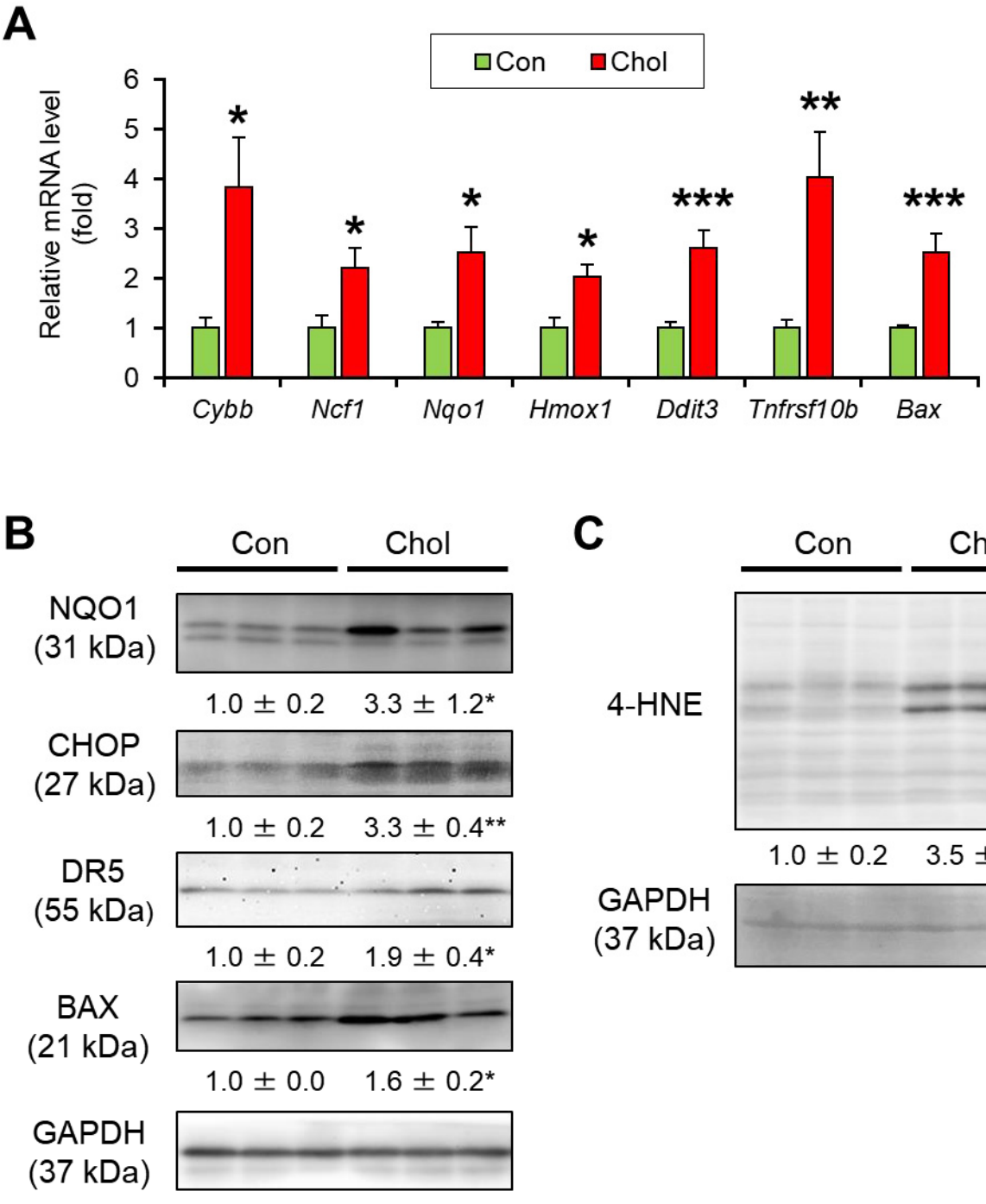
A
Con
Chol
Relative mRNA level (fold)
0
1
2
3
4
5
6
*
*
*
*
***
**
***
Cybb
Ncf1
Nqo1
Hmox1
Ddit3
Tnfrsf10b
Bax
B
Con
Chol
NQO1 (31 kDa)
1.0 ± 0.2
3.3 ± 1.2*
CHOP (27 kDa)
1.0 ± 0.2
3.3 ± 0.4**
DR5 (55 kDa)
1.0 ± 0.2
1.9 ± 0.4*
BAX (21 kDa)
1.0 ± 0.0
1.6 ± 0.2*
GAPDH (37 kDa)
C
Con
Chol
4-HNE
1.0 ± 0.2
3.5 ± 0.1***
GAPDH (37 kDa)

Fig. 5. Increased hepatocyte proliferation in the liver of HCVcpTg transgenic mice after a 15-month high-cholesterol diet.

(A) qPCR analysis of genes associated with oncogenic signaling.

(B) Immunoblot analysis of PCNA. Whole liver homogenates (45 μg of protein) were loaded into each well. The bands of GAPDH were used as the loading control. Band intensities were measured densitometrically, normalized to those of the loading control, and expressed as values relative to those of control diet mice. Results were obtained from two independent immunoblot experiments.

(C) PCNA immunostaining. Arrowheads indicate PCNA-expressing hepatocyte nuclei. Bar = 40 μm (200x magnification).

(D) qPCR analysis of genes associated with stemness and epithelia-to-mesenchymal transition.

All mRNA levels were normalized to 18S mRNA levels and subsequently expressed as values relative to those of control diet mice. Values are expressed as the mean ± SEM. $*P < 0.05$, $**P < 0.01$ between control diet and high-cholesterol diet HCVcpTg mice.

Figure 5

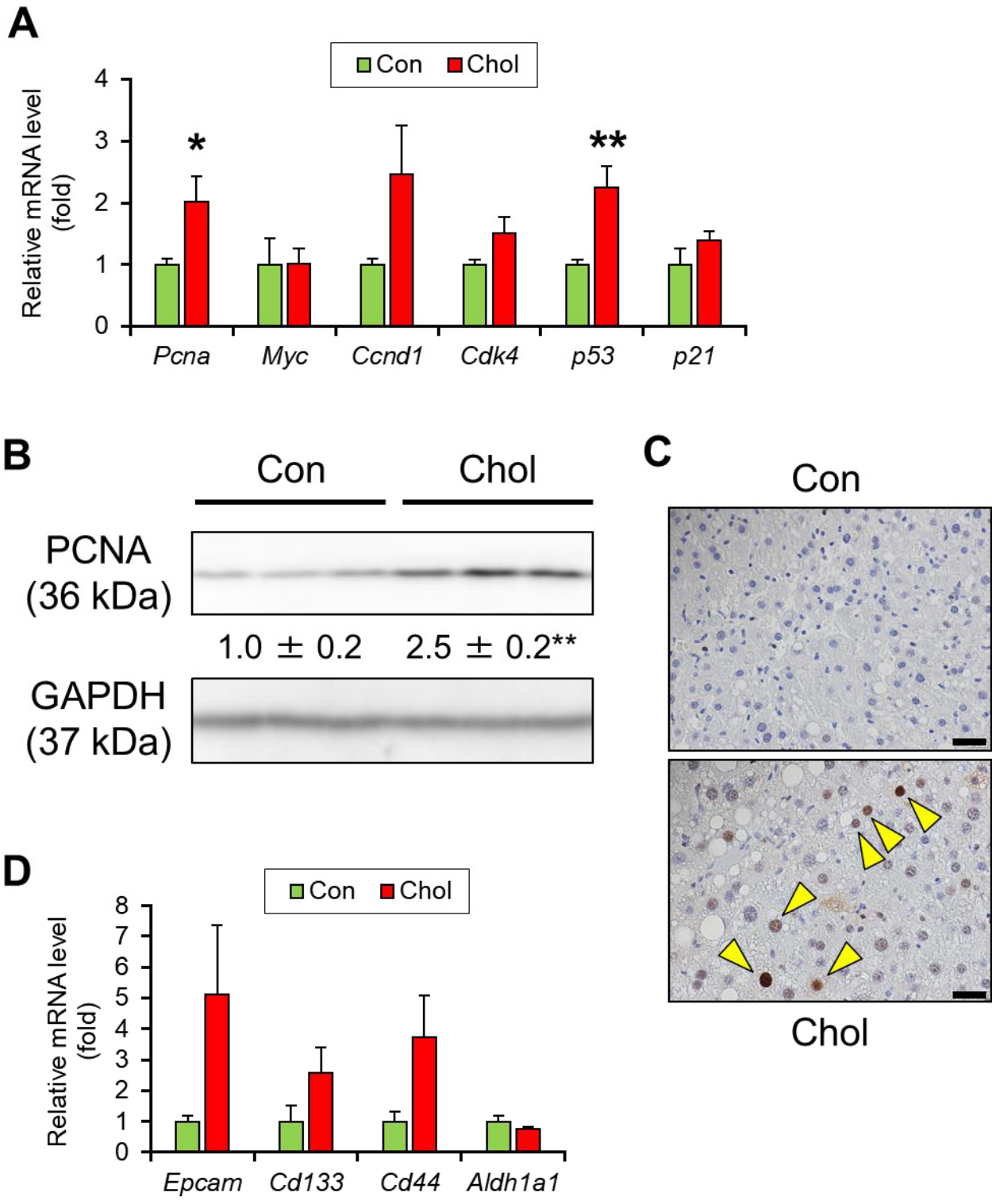
A
Con
Chol
Relative mRNA level (fold)
0
1
2
3
4
*
**
Pcna
Myc
Ccnd1
Cdk4
p53
p21
B
Con
Chol
PCNA (36 kDa)
1.0 ± 0.2
2.5 ± 0.2**
GAPDH (37 kDa)
C
Con
Chol
D
Con
Chol
Relative mRNA level (fold)
0
1
2
3
4
5
6
7
8
Epcam
Cd133
Cd44
Aldh1a1

Fig. 6. Marked up-regulation of the p62/Sqstm1-NRF2 axis in the liver of HCVcpTg transgenic mice after a 15-month high-cholesterol diet.

(A) qPCR analysis of *Sqstm1* (encoding p62 protein) and *Nfe2l2* (encoding NRF2 protein) genes. All mRNA levels were normalized to 18S mRNA levels and subsequently expressed as values relative to those of control diet mice.

(B and C) Immunoblot analysis of p62 and NRF2 (B) and nuclear NRF2 (C). The same samples respectively used in Fig. 4B (whole liver lysates, 45 μg of protein) and 2B (nuclear fractions, 20 μg of protein) were loaded into each well. Band intensities were measured densitometrically, normalized to those of the loading control, and expressed as values relative to those of control diet mice. Results were obtained from two independent immunoblot experiments.

Values are expressed as mean ± SEM. $*P < 0.05$, $**P < 0.01$, $***P < 0.001$ between control diet and high-cholesterol diet HCVcpTg mice.

(D) Proposed mechanism of how long-term excessive cholesterol intake promotes liver tumorigenesis in HCVcpTg mice.

Figure 6

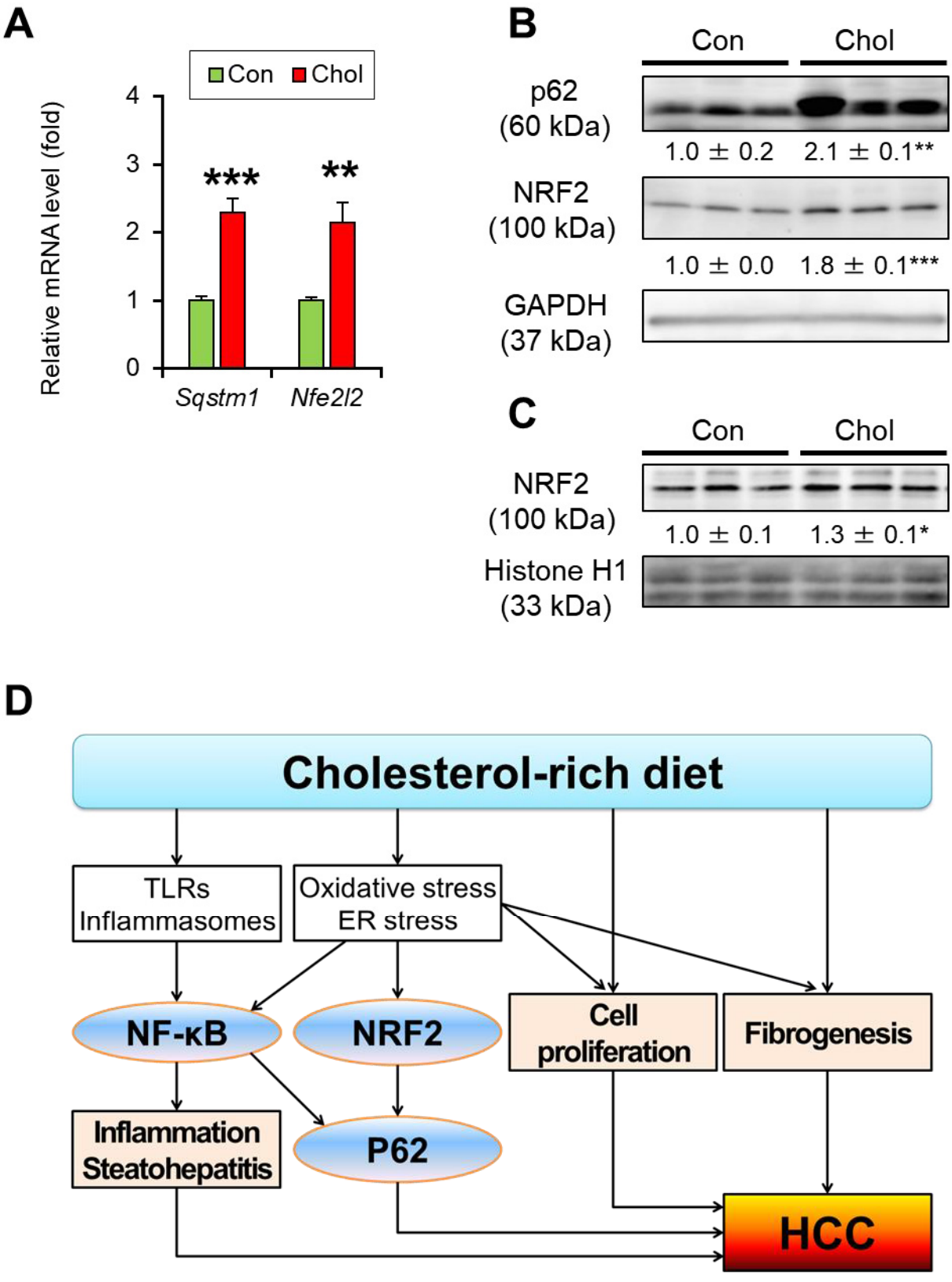
A
Con
Chol
Relative mRNA level (fold)
4
3
2
1
0
***
**
Sqstm1
Nfe2l2
B
Con
Chol
p62
(60 kDa)
1.0 ± 0.2
2.1 ± 0.1**
NRF2
(100 kDa)
1.0 ± 0.0
1.8 ± 0.1***
GAPDH
(37 kDa)
C
Con
Chol
NRF2
(100 kDa)
1.0 ± 0.1
1.3 ± 0.1*
Histone H1
(33 kDa)
D
Cholesterol-rich diet
TLRs
Inflammasomes
Oxidative stress
ER stress
NF-κB
NRF2
Cell
proliferation
Fibrogenesis
Inflammation
Steatohepatitis
P62
HCC

References

1. Kimura T, Tanaka N, Fujimori N, et al. Mild drinking habit is a risk factor for hepatocarcinogenesis in non-alcoholic fatty liver disease with advanced fibrosis. World J Gastroenterol. 2018;24: 1440-1450.
2. Kimura T, Kobayashi A, Tanaka N, et al. Clinicopathological characteristics of non-B non-C hepatocellular carcinoma without past hepatitis B virus infection. Hepatol Res 2017; 47: 405-418.
3. Yoshimoto S, Loo TM, Atarashi K, et al. Obesity-induced gut microbial metabolite promotes liver cancer through senescence secretome. Nature 2013; 499(7456): 97-101.
4. Tall AR, Yvan-Charvet L. Cholesterol, inflammation and innate immunity. Nat Rev Immunol. 2015;15: 104-116.
5. Silva Afonso M, Marcondes Machado R, Ferrari Lavrador MS, Carlos Rocha Quintao E, Moore KJ, Lottenberg AM. Molecular Pathways Underlying Cholesterol Homeostasis. Nutrients. 2018;10.
6. Musso G, Gambino R, Cassader M. Cholesterol metabolism and the pathogenesis of non-alcoholic steatohepatitis. Prog Lipid Res. 2013;52: 175-191.
7. Eckel RH, et al. 2013 AHA/ACC Guideline on Lifestyle Management to Reduce Cardiovascular Risk. Circulation 2014;129(25 Suppl 2):S76-99
8. Ioannou GN, Morrow OB, Connole ML, Lee SP. Association between dietary nutrient composition and the incidence of cirrhosis or liver cancer in the United States population. Hepatology. 2009;50: 175-184.
9. Yu L, Morishima C, Ioannou GN. Dietary cholesterol intake is associated with progression of liver disease in patients with chronic hepatitis C: analysis of the Hepatitis C Antiviral Long-term Treatment Against Cirrhosis trial. Clin Gastroenterol Hepatol. 2013;11:1661-1666.
10. Moriya K, Fujie H, Shintani Y, et al. The core protein of hepatitis C virus induces hepatocellular carcinoma in transgenic mice. Nat Med. 1998;4: 1065-1067.
11. Koike K, Moriya K, Ishibashi K, et al. Expression of hepatitis C virus envelope proteins in transgenic mice. J Gen Virol. 1995;76 (Pt 12): 3031-3038.
12. Tanaka N, Moriya K, Kiyosawa K, Koike K, Aoyama T. Hepatitis C virus core protein induces spontaneous and persistent activation of peroxisome proliferator-activated receptor alpha in transgenic mice: implications for HCV-associated hepatocarcinogenesis. Int J Cancer. 2008;122: 124-131.
13. Tanaka N, Moriya K, Kiyosawa K, Koike K, Gonzalez FJ, Aoyama T. PPARalpha activation is essential for HCV core protein-induced hepatic steatosis and hepatocellular carcinoma in mice. J Clin Invest. 2008;118: 683-694.
14. Lu Y, Harada M, Kamijo Y, et al. Peroxisome proliferator-activated receptor α attenuates high-cholesterol diet-induced toxicity and pro-thrombotic effects in mice. Arch Toxicol. 2019;93:149-161.
15. Hu X, Tanaka N, Guo R, et al. PPARalpha protects against trans-fatty-acid-containing diet-induced steatohepatitis. J Nutr Biochem. 2017;39: 77-85.
16. Tanaka N, Matsubara T, Krausz KW, Patterson AD, Gonzalez FJ. Disruption of

phospholipid and bile acid homeostasis in mice with nonalcoholic steatohepatitis. Hepatology. 2012;56: 118-129.
17. Tanaka N, Takahashi S, Fang ZZ, et al. Role of white adipose lipolysis in the development of NASH induced by methionine- and choline-deficient diet. Biochim Biophys Acta. 2014;1841: 1596-1607.
18. Karasawa F, Shiota A, Goso Y, et al. Essential role of gastric gland mucin in preventing gastric cancer in mice. J Clin Invest. 2012;122:923-934.
19. Tanaka N, Takahashi S, Zhang Y, et al. Role of fibroblast growth factor 21 in the early stage of NASH induced by methionine- and choline-deficient diet. Biochim Biophys Acta_Molecular Basis of Disease 2015; 1852: 1242-1252.
20. Tanaka N, Takahashi S, Matsubara T, et al. Adipocyte-specific disruption of fat-specific protein 27 causes hepatosteatosis and insulin resistance in high-fat diet-fed mice. J Biol Chem 2015; 290: 3092-3105.
21. Nagaya T, Tanaka N, Suzuki T, et al. Down-regulation of SREBP-1c is associated with the development of burned-out NASH. J Hepatol 2010; 53: 724-731.
22. Jain A, Lamark T, Sjottem E, et al. p62/SQSTM1 is a target gene for transcription factor NRF2 and creates a positive feedback loop by inducing antioxidant response element-driven gene transcription. J Biol Chem. 2010;285: 22576-22591.
23. Umemura A, He F, Taniguchi K, et al. p62, Upregulated during Preneoplasia, Induces Hepatocellular Carcinogenesis by Maintaining Survival of Stressed HCC-Initiating Cells. Cancer Cell. 2016;29: 935-948.
24. Loguercio C, Federico A, Masarone M, Torella R, Blanco Cdel V, Persico M. The impact of diet on liver fibrosis and on response to interferon therapy in patients with HCV-related chronic hepatitis. Am J Gastroenterol. 2008;103: 3159-3166.
25. Yu L, Morishima C, Ioannou GN. Dietary cholesterol intake is associated with progression of liver disease in patients with chronic hepatitis C: analysis of the hepatitis C antiviral long-term treatment against cirrhosis trial. Clinical Gastroenterology and Hepatology. 2013;11: 1661-1666. e1663.
26. Yu L, Morishima C, Ioannou GN. Sex difference in liver-related mortality and transplantation associated with dietary cholesterol in chronic hepatitis C virus infection. British Journal of Nutrition. 2016;115: 193-201.
27. Tanaka N, Aoyama T, Kimura S, Gonzalez FJ. Targeting nuclear receptors for the treatment of fatty liver disease. Pharmacol Ther. 2017;179: 142-157.
28. Moriishi K, Mochizuki R, Moriya K, et al. Critical role of PA28gamma in hepatitis C virus-associated steatogenesis and hepatocarcinogenesis. Proc Natl Acad Sci U S A. 2007;104: 1661-1666.
29. Yamashita T, Honda M, Takatori H, et al. Activation of lipogenic pathway correlates with cell proliferation and poor prognosis in hepatocellular carcinoma. J Hepatol. 2009;50: 100-110.
30. Wu H, Ng R, Chen X, Steer CJ, Song G. MicroRNA-21 is a potential link between non-alcoholic fatty liver disease and hepatocellular carcinoma via modulation of the HBP1-p53-Srebp1c pathway. Gut. 2015: gutjnl-2014-308430.
31. Ogura S, Yoshida Y, Kurahashi T, et al. Targeting the mevalonate pathway is a novel therapeutic approach to inhibit oncogenic FoxM1 transcription factor in human

hepatocellular carcinoma. Oncotarget. 2018;9: 21022.
32. Liu D, Wong CC, Fu L, et al. Squalene epoxidase drives NAFLD-induced hepatocellular carcinoma and is a pharmaceutical target. Sci Transl Med. 2018;10(437).
33. Liang JQ, Teoh N, Xu L, et al. Dietary cholesterol promotes steatohepatitis related hepatocellular carcinoma through dysregulated metabolism and calcium signaling. Nat Commun. 2018;9(1):4490.
34. Marí M, Caballero F, Colell A, et al. Mitochondrial free cholesterol loading sensitizes to TNF-and Fas-mediated steatohepatitis. Cell Metab. 2006;4: 185-198.
35. Gan LT, Van Rooyen DM, Koina ME, McCuskey RS, Teoh NC, Farrell GC. Hepatocyte free cholesterol lipotoxicity results from JNK1-mediated mitochondrial injury and is HMGB1 and TLR4-dependent. J Hepatol. 2014;61: 1376-1384.
36. Saito T, Ichimura Y, Taguchi K, et al. p62/Sqstm1 promotes malignancy of HCV-positive hepatocellular carcinoma through Nrf2-dependent metabolic reprogramming. Nature communications. 2016;7: 12030.
37. Simon Y, Kessler SM, Bohle RM, Haybaeck J, Kiemer AK. The insulin-like growth factor 2 (IGF2) mRNA-binding protein p62/IGF2BP2-2 as a promoter of NAFLD and HCC? Gut. 2014;63: 861-863.
38. Tanaka N, Takahashi S, Hu X, et al. Growth arrest and DNA damage-inducible 45α protects against nonalcoholic steatohepatitis induced by methionine- and choline-deficient diet. Biochim Biophys Acta Mol Basis Dis. 2017;1863(12):3170-3182.
39. Tanaka N, Kimura T, Fujimori N, Nagaya T, Komatsu M, Tanaka E. Current status, problems, and perspectives of non-alcoholic fatty liver disease research. World J Gastroenterol. 2019;25(2):163-177.
40. You Q, Cheng L, Kedl RM, Ju C. Mechanism of T cell tolerance induction by murine hepatic Kupffer cells. Hepatology. 2008;48: 978-990.
41. Leroux A, Ferrere G, Godie V, et al. Toxic lipids stored by Kupffer cells correlates with their pro-inflammatory phenotype at an early stage of steatohepatitis. J Hepatol. 2012;57: 141-149.
42. Teratani T, Tomita K, Suzuki T, et al. A high-cholesterol diet exacerbates liver fibrosis in mice via accumulation of free cholesterol in hepatic stellate cells. Gastroenterology. 2012;142: 152-164 e110.